

Development and Evaluation of a Photochemical Chamber to Examine the Toxicity of Coal-Fired Power Plant Emissions

Pablo A. Ruiz, Joy E. Lawrence, Jack M. Wolfson, Stephen T. Ferguson, Tarun Gupta, Choong-Min Kang, and Petros Koutrakis

Exposure, Epidemiology, and Risk Program, Department of Environmental Health, Harvard School of Public Health, Boston, Massachusetts, USA

When investigating the toxicity of individual particle sources, it is important to consider the contribution of both primary and secondary particles. In this article, we present the design of a new photochemical chamber that can be used to form secondary sulfuric acid particles from diluted coal-fired power plant emissions. The chamber is a relatively small, well-mixed flow reactor that can fit in a mobile reaction laboratory. It produces high concentrations of hydroxyl radical (OH) from the photolysis of ozone (O₃) in the presence of water vapor. Two chambers were built and tested. A pilot chamber was tested in the laboratory, using mixtures of NO and SO₂ in air, at concentrations that are approximately 100 times lower than those in power plant stack emissions. This chamber was able to oxidize about 20% of the SO₂, thereby producing 1350 μg m⁻³ of H₂SO₄ particles. Further tests showed that increasing O₃ concentrations and residence time increased the H₂SO₄ production. A field chamber was built subsequently and used in a toxicological study. Diluted coal-fired power plant emissions were introduced in the chamber. Over 19 days of exposure, the chamber, on average, converted 17% of the supplied SO₂ emissions and produced an average of 350 μg m⁻³ of H₂SO₄ particles. Particle losses were determined for the pilot chamber, using artificial particles whose size ranged from 50 to 1000 nm. The determined losses ranged from 21 to 42%, with no trend between the amount of particle loss and particle size. Losses for the field chamber, estimated using model calculations, were found to be similar to those of the pilot chamber.

Exposures to high levels of ambient particles have been associated with adverse health effects, including cardiopulmonary

mortality and morbidity (Dockery et al., 1993; Dockery & Pope, 1994; Pope et al., 1995). The particles responsible for these associations originate from a variety of sources, such as coal- and oil-fired power plants and motor vehicles. Because the composition and physicochemical characteristics of the particles vary greatly, depending upon the source, it is expected that their toxicity also should differ greatly.

Received 1 August 2006; accepted 5 February 2007.

This project was supported by the Electric Power Research Institute (contract EP-P10983/C5530/56546); the U.S. Environmental Protection Agency; the PM Center at the Harvard School of Public Health (grant R827 353-01-0); and the Harvard NIEHS Center for Environmental Health (grant ES00002). This work also was conducted with the support of the U.S. Department of Energy (DOE), under award DE-FC26-03NT41902. However, any opinions, findings, conclusions, or recommendations expressed herein are those of the authors and do not necessarily reflect the views of the DOE. We thank the EPRI project manager, Dr. Annette Rohr, for her interest, interaction, and suggestions. Also, we thank Dr. John Godleski and Dr. Stephen Rudnick for reading the manuscript and providing helpful suggestions. We also acknowledge the efforts of Mark Davey, Denise Lamoureux, and Erick Vlassidis for laboratory and analytical support; and, finally, we thank all the people who helped with the field tests at the power plant.

Address correspondence to Pablo A. Ruiz, Exposure, Epidemiology, and Risk Program, Department of Environmental Health, Harvard School of Public Health, 401 Park Drive, Boston, MA 02215, USA. E-mail: pruiz@hsph.harvard.edu

Researchers have studied the toxicity of source emissions by exposing subjects to particles representative of these sources. A frequently used approach is to use direct diluted emissions. For instance, emissions from mobile sources have been tested using motor vehicles running in dynamometers (McDonald et al., 2004; Reed et al., 2004). For the case of oil and coal-fired power plants, particle emissions have been studied mainly using resuspended fly ash as emissions surrogates (Kodavanti et al., 1998, 2002; Wellenius et al., 2002). However, these studies only consider the effect of directly emitted particles, whereas ambient particles are a mixture of both directly emitted particles (primary) and particles formed in the atmosphere through atmospheric reactions (secondary).

For the case of coal-fired power plants, primary emissions comprise both particles and gases. A major component of the gas emissions is sulfur dioxide (SO_2). In the plume, SO_2 is oxidized, forming secondary sulfuric acid particles (H_2SO_4). This reaction can change the content and composition of the particle phase, and as such, it can potentially greatly change the toxicity of the emissions. Further plume reactions can additionally change the toxicity of these emissions. For instance, the aerosol may be neutralized by ammonia (NH_3), thereby changing its acidity. Additionally, once the plume reaches an urban population, the emissions could be mixed with particles from other sources.

To realistically investigate particle toxicity from individual sources, we have developed a comprehensive approach. In this approach emissions from an individual source are sampled and diluted in situ, and then atmospheric reactions are simulated using reaction chambers. Animals are exposed to the thus generated aerosols. This approach was used to develop a complete exposure system that can be used to study coal-fired power plant emissions (Ruiz et al., 2007). As part of the system it was necessary to develop reaction chambers to simulate key atmospheric reactions.

It is the objective of this article to present the design and evaluation of a photochemical chamber that simulates a key plume reaction: the oxidation of SO_2 to form H_2SO_4 particles. To simulate other atmospheric reactions, our system includes a second chamber that is described elsewhere (Ruiz et al., 2007). There are two major challenges for a chamber to be used in our system. First, it should be adequate to be used in field experiments conducted at a power plant, and second, it should produce the test aerosol within a short preparation time. In the past, plume reactions from power plant emissions, including SO_2 oxidation, have been simulated using smog chambers (Luria et al., 1982, 1983). However, the smog chambers used in those studies have features that limit their applicability in our system: They usually are large, which makes them impractical for use at a power plant; they operate as batch reactors, which results in exposures that vary over time; and finally, they usually rely on solar light, which changes with time of day and meteorological conditions.

As an alternative, in this article we present a new, relatively small photochemical chamber that can fit easily inside a mobile reaction laboratory the size of a minibus. It uses special ultraviolet lamps to drive photochemical reactions at a high rate, producing stable concentrations of sulfuric acid in a relatively short preparation time period. Two chambers were built and tested. A first, pilot chamber was tested in the laboratory with artificial gas mixtures. A second, field chamber was built and tested using real, diluted power plant emissions.

METHODS

Reactions

In the atmosphere, SO_2 is oxidized by reacting with hydroxy radicals (OH) (Stockwell & Calvert, 1983). For a chamber to oxidize SO_2 at a high rate it must produce high concentrations

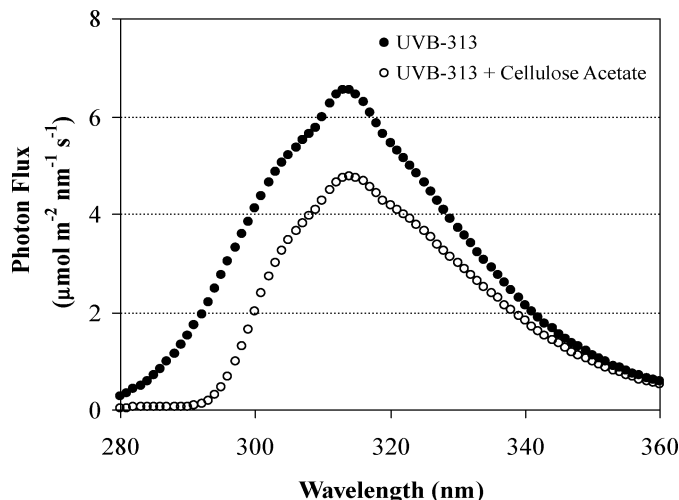


FIG. 1. Emission spectra of UVB-313 lamps: alone and covered with cellulose acetate film.

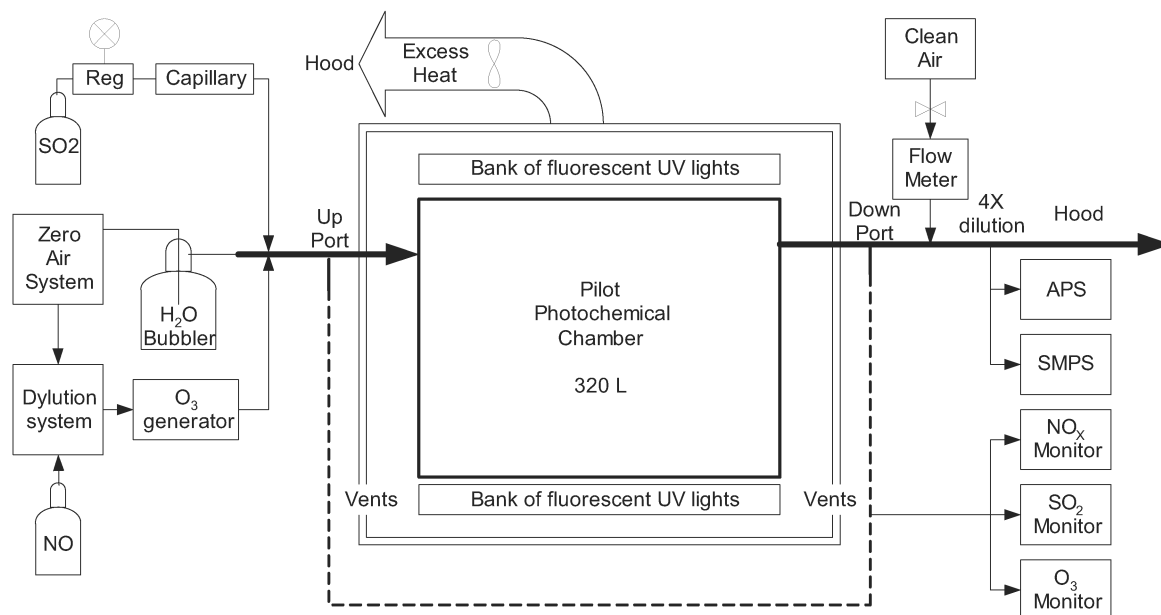
of OH. This radical can be produced, via a series of reactions, from the photolysis of O_3 . When O_3 is photolyzed by light of a sufficiently short wavelength (<336 nm), an electronically excited form of oxygen [$\text{O}(^1\text{D})$] is formed, which can then react with water vapor, forming OH. Thus, the SO_2 of the emissions can be oxidized by mixing the diluted emissions with excess O_3 and water vapor, and exposing the mixture to special lights. To succeed, the rate of OH generation should be proportional to the input rate of SO_2 . It should also be considered that nitrogen oxides, also released by the power plants, compete with SO_2 for OH (Hewitt, 2001; Seinfeld & Pandis, 1998), thus increasing the requirement for OH generation.

To enhance OH production, so that a relatively small chamber could be used, we used lamps that greatly enhance the photolysis of O_3 (UVB-313 lamps, Q-Panel Lab Products, Cleveland, OH). These lamps have a light spectrum with a strong photon emission below 330 nm, as shown in Figure 1. Light spectra were acquired with a spectroradiometer (model SPEC UV/PAR, Apogee Instruments, Inc., Logan, UT). However, they also provide light of wavelengths below 295 nm, which are not present in the solar spectrum at ground level (Finlayson-Pitts & Pitts, 2000). To avoid possible artifact reactions, we used a 127- μm -thick cellulose acetate film as a light filter (Holmes, 2002; Mcleod, 1997). This filter was able to remove light of wavelengths below 295 nm from the lamps emissions, as shown in Figure 1.

Chamber and Apparatus for Laboratory Evaluation

The pilot chamber was built as a rectangular (320 L) box of 120 × 80 × 33 cm (L × W × H). For walls, we used 51- μm -thick fluorinated ethylene propylene (FEP) Teflon film (American Durafilm, Holliston, MA) to both minimize wall reactions and allow light transmission (Cocker et al., 2001). Walls were supported by a rigid structural framework, in such a way that only Teflon surfaces faced the interior. Teflon fittings were

a.



b.

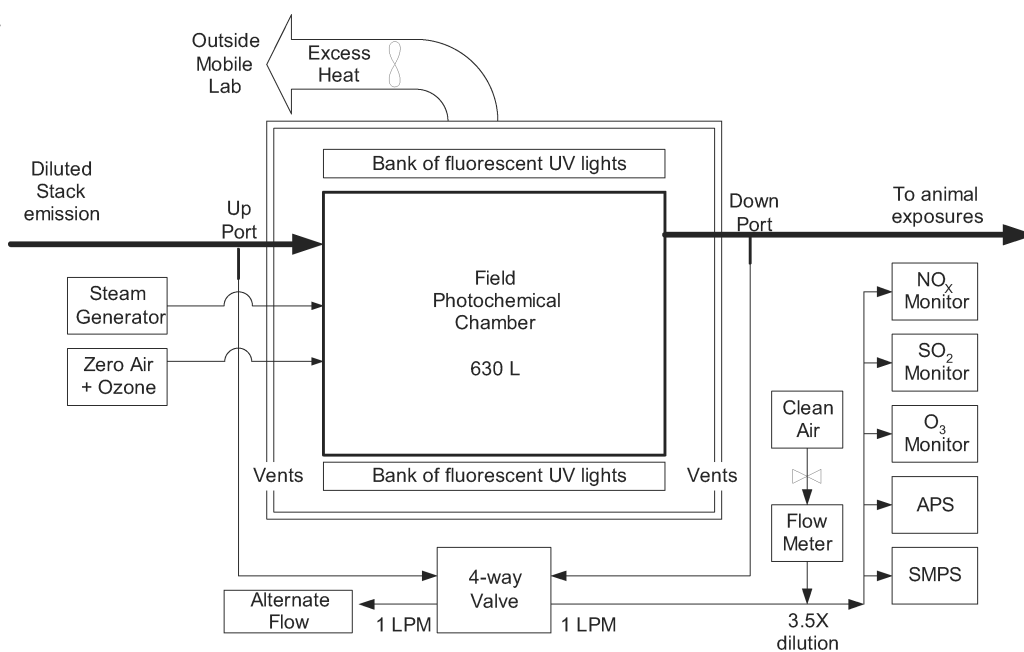


FIG. 2. Schematic of apparatus for the different experiments: (a) pilot chamber performance using a simulated emission; (b) field chamber performance using a real diluted emission.

placed at each end, as inlets and outlets. Banks of lamps were placed above and below the chamber, at a distance of 1 to 2 cm from the walls. The chamber and lamps were enclosed in an opaque, ventilated box to both protect personnel from ultraviolet (UV) light exposure and keep the temperature controlled when the lamps were on. The temperature in the enclosure was

monitored by means of a thermo-hygrometer sensor (model 411, Omega Engineering Inc., Stamford, CT).

The apparatus for laboratory tests is shown in Figure 2a. A manifold was placed at the inlet of the chamber, where a flow of humid air was mixed with a flow of dry air carrying the reactant gases. The mixing of both flows had an H_2O vapor concentration

of $0.56 \mu\text{mol cm}^{-3}$. The humid flow was produced by bubbling clean air in ultrapure water. Clean air was produced by passing room air through consecutive cylinders of silica gel (to remove water), Hydrosil (activated alumina coated with KMnO_4 , to remove oxidizable gases), activated carbon (to remove volatile organic compounds, VOCs), and Hopcalite (a mixture of Mn and Cu oxides, to remove CO), and finally through a particle filter. The dry flow carrying the gases was prepared by mixing clean air first with NO, using a dynamic gas dilution/titration system (TEI model 146C, Franklin, MA), and with SO_2 using a capillary and a pressure regulator. NO and SO_2 were supplied from certified tanks (Matheson Tri-Gas, Montgomeryville, PA). Finally, O_3 was added, before adding SO_2 , by exposing the dry flow to five consecutive ozonator lamps (model 97-0067-01, UVP, Inc., Upland, CA).

Concentrations entering and leaving the chamber were monitored, using continuous gas and particle monitors. O_3 was monitored by UV photometry (TEI model 49C, Franklin, MA), NO and NO_2 by chemiluminescence (TEI model 42C), and SO_2 by pulsed fluorescence (TEI model 43C). Particle concentrations and size distributions were monitored every 5 min by means of a scanning mobility particle sizer (SMPS model 3934, TSI, Inc., Shoreview, MN) and an aerodynamic particle sizer (APS model 3321, TSI, Inc.). To reduce aerosol consumption, particle air samples were diluted by a factor of 4 and particle monitors used filtered room air as sheath air.

SMPS reported particle electrical mobility diameters (d_{me}) between 0.013 and $0.700 \mu\text{m}$, while APS reported particle aerodynamic diameters (d_a) between 0.5 and $20 \mu\text{m}$. For the SMPS, d_{me} was assumed to be the same as the equivalent diameter (d_e); for APS data, the aerodynamic diameter was converted to d_e using the following equation (Peters et al., 1993):

$$d_e = d_a \sqrt{\frac{C_a \chi \rho_0}{C_e \rho_p}} \quad [1]$$

where C_a and C_e are the slip correction factors for d_a and d_e , respectively; ρ_p and ρ_0 are particle and water density, respectively; and χ is the shape factor. Particle density was estimated assuming that particles were comprised of H_2SO_4 and bound water. For simplicity, we assumed the density to be 1.4 g cm^{-3} , the average of the densities of H_2SO_4 (1.8 g cm^{-3}) and H_2O (1 g cm^{-3}). The shape factor was assumed to be 1 (representing a sphere), as expected for liquid particles. Particle mass concentrations (C_m) were calculated using particle equivalent diameter, density, volume, and particle number concentrations. To cover the full range of diameters and to avoid overlapping in the measurements of both instruments, SMPS measurements were used for particles below $0.5 \mu\text{m } d_e$, and APS for particles above $0.5 \mu\text{m } d_e$.

Average particle size was calculated from the aerosol size distribution. Because the produced aerosols will be used in toxicological studies, when calculating an average particle size, it is important to give more weight to the particles that

provide more mass. Hence, the geometric mass mean diameter (GMMD) was calculated using Eq. (2) and used as a measure of average particle size,

$$\text{GMMD} = \exp \left[\frac{\sum n_i d_i^3 \ln d_i}{\sum n_i d_i^3} \right] \quad [2]$$

where n_i and d_i are the number concentration and size diameter, respectively, for size interval i .

In addition to continuous sampling, integrated samples were also collected downstream of the chamber, using 47-mm Teflon membrane filters (R2PJ047, Pall Life Sciences, East Hills, NY). Sulfate concentrations were determined from aqueous extracts of the Teflon filters, using an ion chromatograph (DX 120, Dionex Corporation, Sunnyvale, CA) as described before (Koutrakis et al., 1988).

Particle losses were determined using a slight modification of the previous apparatus. Monodisperse artificial particles (Carboxylate Microspheres, Polybeads, Polysciences Inc., Warrington, PA) were produced using a Lovelace nebulizer (Intox Products, Moriarity, NM) operated at 35 psi. Droplets of ammonia solution were added to the particle suspension to avoid agglomerations. The 2.5 lpm output of the nebulizer was diluted with dry clean air. From this flow, 0.5 lpm were taken and passed through a citric acid diffusion denuder, followed by a radioactive neutralizer (model 3012, TSI, Inc., Shoreview, MN), and then diluted to 5 lpm using clean air with the relative humidity (RH) adjusted to 64%. This test aerosol was introduced in the inlet of the chamber for 3 h (about 3 residence times), and then the particle size distributions upstream and downstream of the chamber were measured for about 2 to 3 h using the APS and SMPS. Particle losses were calculated using Eq. (3):

$$\text{Losses (\%)} = 100 \times \left(1 - \frac{C_{down}}{C_{up}} \right) \quad [3]$$

where C_{up} and C_{down} are average particle concentrations upstream and downstream of the chamber, respectively.

Chamber and Apparatus for Field Evaluation

Following laboratory evaluation of the pilot chamber, a more rugged chamber suitable for field work was designed and manufactured in a machine shop (Boston University, Boston). This 630-L chamber was a rectangular, sealed aluminum framework with inner dimensions of $150 \times 35 \times 120 \text{ cm}$ (L \times W \times H), with the larger sides of the framework left open for irradiation. To avoid wall reactions, the inner surfaces of the aluminum frame were covered with PTFE Teflon sheets; meanwhile, the open sides of the chamber were covered with Teflon films. In this way, only Teflon surfaces were exposed to the chamber interior. Stainless-steel bulkhead fittings (2.54 mm ID) were placed at both ends of the chamber and used as inlet and outlet ports. The chamber was placed inside a ventilated wood enclosure, with banks of UVB-313 lamps and cellulose acetate placed on the enclosure sides at a distance of about 10 cm from the chamber

walls. The enclosure, including the chamber and lamps, was placed inside a minibus (Allstar series 20 passenger bus, Starcraft Bus, Goshen, IN) modified as a mobile reaction laboratory, including custom equipment for ventilation and temperature control.

The apparatus for the field evaluation is shown in Figure 2b. Details of the power plant, sampling and dilution technique, and the method used to deliver the diluted sample of stack emissions to the chamber are described elsewhere (Ruiz et al., 2007). The chamber was fed with a constant flow of the diluted emissions, and mixed with both a flow of clean air carrying O₃ and water vapor. Ozone was produced by six consecutive ozonator lamps. The sum of the diluted emissions and ozone flows always was 7 lpm. Water vapor was added directly into the chamber as steam. This was done by pushing ultrapure water, by means of a syringe pump, through two stainless-steel tubes heated with an electrical element.

Pollutants entering and leaving the chamber were continuously monitored in two ports using the same instruments as the laboratory evaluation. At these ports, a flow of 1 lpm always was collected. Only one of the flows was analyzed at a time, and the other was dumped. Upstream and downstream measurements were switched automatically, every 20 min, using an automatic 4-way valve. Measurements downstream of the chamber were not always available because in some cases monitors were sampling other sections of our system. Before the monitors, the sample flow was diluted by a factor of 3.5 with clean air. Temperature and RH were monitored using a Vaisala transmitter (HMD-70, Vaisala Oyj, Helsinki, Finland) placed inside the enclosure. A flow of 0.3 L/min was taken from the chamber and passed through the sensor.

Procedures

NO₂ photolysis rates for the chambers were determined by steady-state actinometry (Cocker et al., 2001). To do this, a mixture of NO₂ in air was passed through the chamber until stable concentrations were reached. Then, lights were turned on and, after the concentration reached steady-state, the NO₂ photolysis rate (j_1) was calculated using Eq. (4):

$$j_1 = \frac{k_2[\text{NO}][\text{O}_3]}{[\text{NO}_2]} \quad [4]$$

where k_2 is the rate constant of the reaction of NO with O₃.

The ability of the pilot chamber to oxidize SO₂ was tested, using air mixtures simulating diluted stack emissions. Experiments typically consisted of three stages. First, the chamber was flushed for several hours with dry clean air. Then, the test mixture was passed until chamber concentrations were approximately at steady state (typically after 3 residence times). Finally, reactions were started by turning the UV lamps on. Four experiments were conducted. First, the performance of the chamber was investigated, in detail, using a mixture simulating a representative diluted emission (Experiment A). Then the effects of changing O₃ concentrations (Experiments

B and C) and residence time (Experiments B and D) were investigated.

The ability of the field chamber to produce H₂SO₄ particles, using real diluted stack emissions, was tested at a coal-fired power plant located in the upper Midwest. This study was conducted between April and November 2004, and comprised 5 rounds of exposure of 3 or 4 days each, yielding a total of 19 days of exposure. A typical experiment started with the chamber being flushed overnight with the diluted emissions. At that point, the diluted emissions were mixed with a flow of O₃ in clean air and water vapor, and lamps were turned on. After 5 h of stabilization, exposures took place for 6 h. During this period, sulfate samples were collected downstream of the chamber.

RESULTS AND DISCUSSION

The general objectives of the laboratory evaluation were (1) to test the conceptual approach, and (2) to qualitatively evaluate the effect of changing some experimental parameters (O₃ concentrations and residence time). The reproducibility of the method was evaluated in a more realistic setting in fieldwork experiments using the exhaust from a coal-fired power plant.

Laboratory Evaluation With Artificial Gas Mixtures

First, we evaluated light irradiation in the pilot chamber by measuring the NO₂ photolysis rate, which was determined to be 0.23 min⁻¹. Then we evaluated whether the chamber behaved as a well-mixed flow reactor. For this type of reactor, it is expected that when flushing a pollutant from the chamber with clean air, the pollutant concentration should decay logarithmically. When the chamber was filled with a mixture of carbon monoxide and then flushed with 5 lpm of clean air, we observed a logarithmic decay of the gas with a rate in agreement with an empirical volume of 350 L.

The ability of the chamber to convert SO₂ to H₂SO₄ particles was tested by challenging the pilot chamber with different artificial gas mixtures. Table 1 shows results for four experimental runs. For the first experiment (A) we used a gas mixture that represented a 100 times dilution of the exhaust from a prospective power plant mixed with excess ozone. Only NO₂ was added as it is expected that once the NO from the emission enters the chamber, all NO will be converted into NO₂. To test for wall losses of gases, we stabilized this mixture in the dark for 3 h. As a result, SO₂ was reduced minimally compared to upstream levels, while NO₂ and O₃ showed significant reductions. Losses of O₃ to the walls were expected. However, for NO₂ it seems more likely that it was transformed to HNO₃ (Mentel et al., 1996; Wahner et al., 1998), and then this gas was removed at the walls.

Photochemical reactions were started by turning lights on. Once reactions started, concentrations of SO₂ decreased exponentially, reaching a steady-state value about 3 h later (Figure 3a). At steady state, the supplied SO₂ concentrations were reduced by 521 ppb (28.6%). At the same time, particle mass concentrations (as measured by the SMPS and the APS) increased, reaching a steady-state value of around 2000 μg m⁻³

TABLE 1
Pilot chamber evaluation using different gas mixtures: Upstream and downstream concentrations and ratios

Parameter	A	B	C	D
Supplied concentration (ppb)				
SO ₂ (ppb)	1821	955	951	960
NO ₂ (ppb)	1254	596	530	576
O ₃ (ppb)	1531	933	1324	937
Downstream concentration, lights off				
SO ₂ (ppb)	1792	869	950	847
NO ₂ (ppb)	703	116	87	508
O ₃ (ppb)	1116	570	1202	536
Downstream concentration, lights on				
SO ₂ (ppb)	1300	693	516	817
NO ₂ (ppb)	937	143	34.5	490
O ₃ (ppb)	1006	724	1188	634
PM ($\mu\text{g m}^{-3}$) ^a	2472	1185	2 343	127 ^b
H ₂ SO ₄ ($\mu\text{g m}^{-3}$)	1367	—	1048	—
Reduction				
SO ₂ (%)	28.9	27.4	45.7	14.9
Conversion				
$\frac{\text{H}_2\text{SO}_4^- \text{ produced (ppb)}}{\text{SO}_2 \text{ supplied (ppb)}} \%$	19.5	—	28.7	—

^aMass concentration is the sum of calculated mass concentrations from SMPS and APS measurements after 2 h of irradiation.

^bConcentration calculated after 1 h of irradiation.

after 2 h of irradiation (Figure 3b). The sharp decrease in total particle mass observed 140 min after irradiation likely was because, at this time, most particles have diameters between 500 and 700 nm, which are not detected well by either the SMPS or the APS (Peters et al., 1993). To confirm the conversion of SO₂ to H₂SO₄ particles, a 1-h filter sample was collected 3 h after irradiation was started. An H₂SO₄ concentration of 1360 $\mu\text{g m}^{-3}$ was observed, which is equivalent to converting 356 ppb (19.5%) of upstream SO₂ into H₂SO₄. This fraction was lower than the observed reduction in SO₂, suggesting that not all of the lost SO₂ was accounted as H₂SO₄, possibly due to wall losses of both SO₂ and H₂SO₄ particles.

The size distribution of the aerosol exiting the chamber was monitored over time. Figures 3c and 3d show the evolution of particle number concentrations and average particle size measured as geometric mass mean diameter (GMMD). Immediately after irradiation, new particles nucleated, thus producing a particle size distribution with a large number (about 1×10^6 counts cm^{-3}) of small particles (about 200 nm GMMD). As time passed, the number concentration of particles decreased steadily, until it stabilized at about 10^4 counts cm^{-3} . At the same time, particles steadily increased in size (Figure 3d), primarily due to condensation of H₂SO₄ over previously formed particles and particle coagulation. After 3 h of irradiation, particle size stabilized at about 700 nm. At this point, we expect that the rate of nu-

cleation of new particles equaled the rate of particle removal due to coagulation, wall losses, and convection out of the chamber.

As an additional laboratory experiment, we tested whether increasing O₃ concentrations increased the production of H₂SO₄ particles. Two experiments (B and C) were run using identical protocols and conditions, except that experiment C examined the effect of higher supplied O₃ concentrations (1324 ppb) than experiment B (933 ppb). After irradiation, SO₂ reduction was higher (435 ppb, 46%) at high O₃ concentrations than at low concentrations (262 ppb, 23%). Additionally, after 2 h irradiation, particle monitors measured higher particle mass concentration ($2343 \mu\text{g m}^{-3}$) at higher O₃ than at lower O₃ concentrations ($1185 \mu\text{g m}^{-3}$), confirming that higher O₃ concentrations increased the oxidation of SO₂.

We also tested whether decreasing the residence time changed the amount of SO₂ conversion. To test this, experiment D was run with the residence time reduced from 64 to 32 min, by increasing the chamber flow rate from 5 to 10 lpm. All other conditions were kept comparable to experiment B. After irradiating the chamber for 1 h (2 residence times), the SO₂ reduction was lower with the shorter residence time (143 ppb, 15%) than with the longer residence time (262 ppb, 27%). Also, particle concentrations were much lower with the shorter residence time ($127 \mu\text{g m}^{-3}$ versus $1185 \mu\text{g m}^{-3}$), demonstrating that a shorter residence time greatly reduces chamber performance.

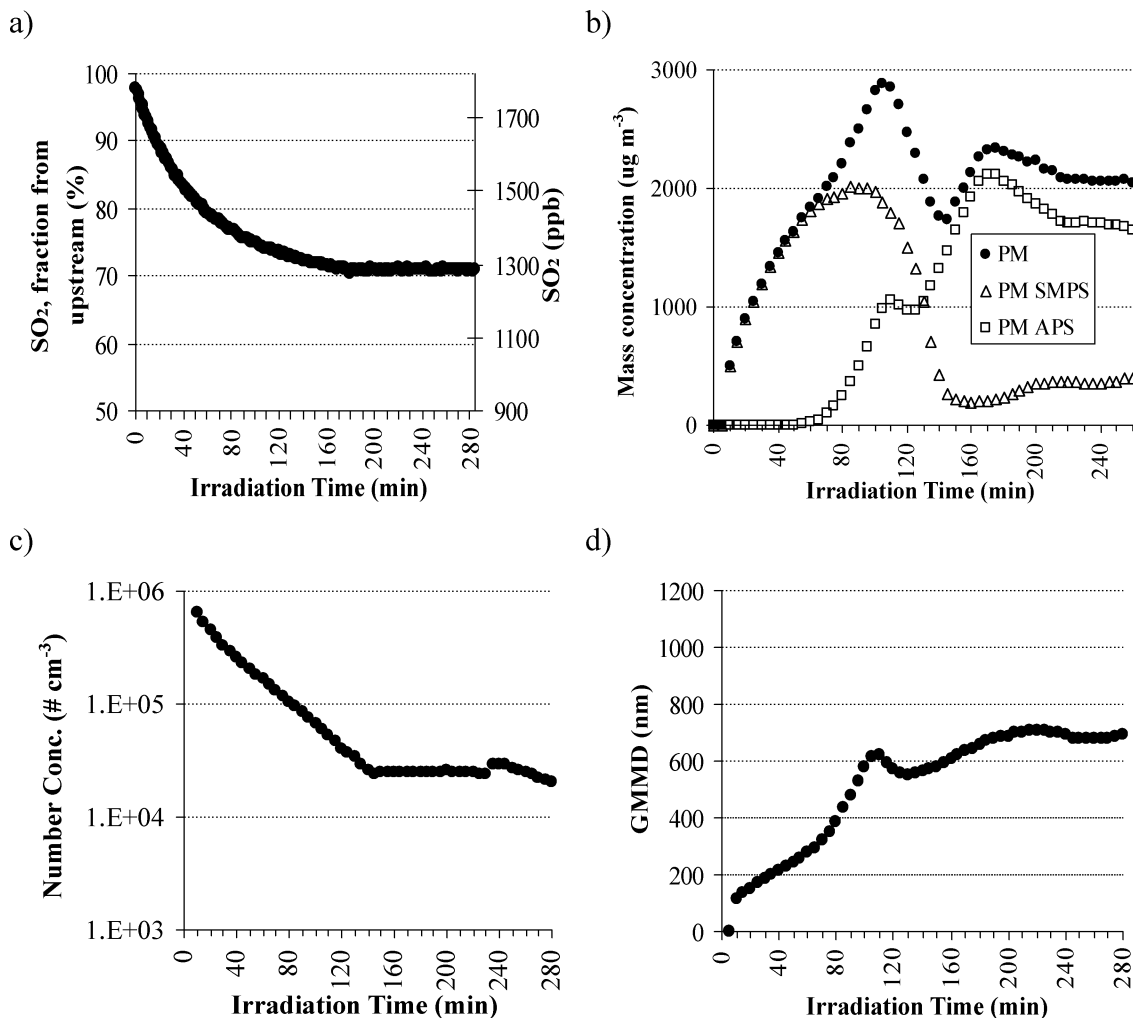


FIG. 3. Performance of the pilot chamber using a SO₂ and NO mixture (experiment A): time evolution of (a) SO₂ concentration, (b) particle mass concentration chamber, (c) particle number concentration, and (d) geometric mass mean diameter (GMMD).

Evaluation in a Field Study at a Power Plant

Initial tests showed that the field chamber presented a NO₂ photolysis rate of 0.096 min⁻¹, about half that observed using the pilot chamber, due mainly to the larger distance between the lamps and chamber walls. To compensate for this reduction in irradiation, the field chamber was operated using a longer residence time (90 min versus the 60 min used with the pilot chamber). As with the pilot chamber, the field chamber was tested to check if it behaved as a well-mixed flow reactor. After passing a mixture of CO in air and flushing with 7 lpm of clean air, a logarithmic decay was observed, with a rate in agreement with an empirical volume of 685 L.

The chamber was used in a toxicological study conducted at a coal-fired power plant. Table 2 shows the results for a total of 19 days of exposure. The pollutant concentrations supplied to the chamber were, on average, 883 ± 210 ppb for NO and 1070 ± 340 ppb for SO₂, with a concentration ratio of NO to SO₂

of 0.85 ± 0.14. Primary emissions have only minor amounts of NO₂. The supplied primary particle concentrations, as measured with the APS and SMPS, were 5.2 ± 6.5 μg m⁻³. During exposures, the percentage of SO₂ reduction was 42.6 ± 17.4%, while NO₂ reduction was 78.8 ± 6.4%. These higher NO₂ losses likely were due to the same mechanism as with the pilot chamber (loss of HNO₃ in the chamber walls). The average H₂SO₄ production in the chamber was 350 ± 153 μg m⁻³. Based on the supplied concentration of SO₂, the average conversion of SO₂ into H₂SO₄ was 16.7 ± 11.3%. The significant percentage of SO₂ reduction that could not be accounted for as H₂SO₄ suggests that, as with the pilot chamber, there were significant wall losses for both SO₂ and H₂SO₄ particles.

For the chamber to successfully simulate plume reactions, it should produce a test aerosol with a realistic ratio of primary to secondary (sulfate) particles. In other words, the fraction of SO₂ converted to H₂SO₄ should be similar to those encountered in

TABLE 2

Field chamber performance: Gas and particle concentrations, removal and conversion ratios, and temperature and humidity conditions

Parameter	<i>n</i>	Average \pm SD
Supplied concentrations		
NO (ppb)	16	884 \pm 210
SO ₂ (ppb)	16	1 071 \pm 341
Ratio NO/SO ₂	16	0.85 \pm 0.14
Primary PM ($\mu\text{g m}^{-3}$) ^a	19	3.4 \pm 3.8
Downstream concentrations		
O ₃ (ppb)	8	422 \pm 166
NO ₂ (ppb)	12	174 \pm 58
SO ₂ (ppb)	12	564 \pm 185
Sulfate ($\mu\text{g m}^{-3}$)	17	350 \pm 153
PM ($\mu\text{g m}^{-3}$) ^a	16	845 \pm 467
Ratios		
SO ₂ reduction (%)	12	42.6 \pm 17.4
$\frac{\text{SO}_4^{2-} \text{ produced (ppb)}}{\text{SO}_2 \text{ supplied (ppb)}} (\%)$	11	16.7 \pm 11.3
Temperature and humidity		
Temperature ($^{\circ}\text{C}$)	16	35.7 \pm 1.7
RH (%)	16	23.1 \pm 2.3
H ₂ O ($\mu\text{mol cm}^{-3}$)	16	0.56 \pm 0.04

^aPM is the sum of APS and SMPS measurements.

typical atmospheres impacted by coal power plants. Considering average plume conversion rates of 1% h⁻¹ (Hewitt, 2001), particles from the chamber were found to be similar to particles generally found in a plume about 18 h after being emitted, which is a reasonable simulation. In future work, if higher sulfate to primary particle ratios were desired, the amount of SO₂ oxidation should be increased. This can be done by increasing the amount of O₃ and/or by increasing the residence time. Additionally, the rate may be increased, if more effective light sources were found.

For animal exposures, it is desirable that the chamber provides an aerosol with a stable size distribution. Size distributions were measured in three experiments. Figure 4 shows the evolution of particle size (GMMD) after irradiation. As with the pilot chamber, initially particles were small (about 100 nm) and then their size increased until a stable size (around 400 to 550 nm) was reached, demonstrating that the chamber can produce test aerosols with stable particle size.

Finally, results from this study should be comparable to previous toxicological studies. Considering the observed sulfate concentrations, and assuming a dilution factor of 6 (aerosol is diluted 6 times with clean air before entering the animal exposure chambers), the expected concentrations for animal exposures would be 58 $\mu\text{g m}^{-3}$. This value is in the range (between 53.1 and 85.2 $\mu\text{g m}^{-3}$) of previous studies that used concentrated urban particles (Batalha et al., 2002; Clarke et al., 2000; Wellenius et al., 2003).

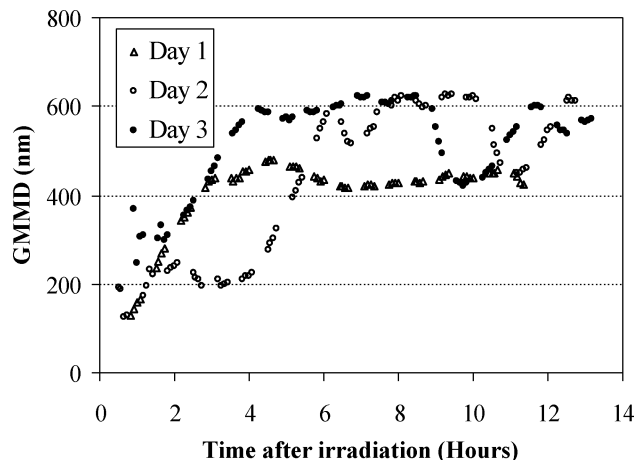


FIG. 4. Particle size evolution in the field chamber after irradiation using a diluted real-life emission: evolution of geometric mass mean diameter (GMMD) as a function of time.

Particle Losses

Particle losses inside the chamber should be minimized. Particle losses were determined experimentally for the pilot chamber by passing artificial monodisperse particles and continuously measuring particles upstream and downstream of the chamber. Table 3 shows the results (average and standard error) for particles of size 50, 100, 500, and 1000 nm. Losses were the lowest (21%) for the 500-nm spheres and highest (42%) for the 100-nm spheres, with no obvious trend between particle size and percentage loss.

For the field chamber losses were not determined experimentally because of logistic infeasibility; but instead, they were estimated from the results of the pilot chamber using a simple box model. For this model, it was assumed the content of the box was well mixed, the air flow coming in equals the air flow coming out, and particles are lost on the walls with a rate that is proportional to both the total internal surface area (*S*) and the particle deposition rate (*u_d*). Assuming this, it can be mathematically derived that the particle concentrations upstream and

TABLE 3
Particle losses for the pilot and field chamber

Particle size (nm)	Losses (%) \pm SE (%)	
	Pilot, experimental	Field, Estimated
50	27.5 \pm 1.1	31.5 \pm 1.3
100	42.4 \pm 0.9	47.2 \pm 1.0
500	23.5 \pm 1.8	23.0 \pm 2.1
1000	37.0 \pm 3.5	42.0 \pm 4.0

downstream of the chamber can be calculated from Eq. (5).

$$\frac{C_{down}}{C_{up}} = \frac{Q}{Q + Su_d} \quad [5]$$

where Q is the flow rate. We assumed that both chambers had similar u_d , since both chambers are well-mixed flow reactors, use similar wall material, have similar geometries and size, and had similar temperatures. Deposition rates for the pilot chamber were calculated using Eq. (5) and the experimental data. Using this approach we found that the estimated losses for the field chamber, shown in Table 3, did not differ much from the those for the pilot chamber.

Overall, we think that for both chambers described here, 30% particle losses are acceptable. As for the mechanism of particle removal, particles are expected to be removed primarily by three main mechanisms. Brownian motion and turbulent diffusion dominates for particles below 100 nm, while gravitational sedimentation dominates for particles over 1 μm in diameter (Crump & Seinfeld, 1981). The third mechanism, electrostatic losses, would be expected for a chamber with non-conductive walls, and dominates for particles between 100 nm and 1 μm (McMurry & Rader, 1985). The observed overall loss rate as a function of particle size is consistent with the three primary removal mechanisms.

CONCLUSIONS

The two chambers described here were shown to be able to oxidize SO_2 from artificial or actual diluted power plant emissions and produce an aerosol adequate for animal exposure (i.e., stable concentrations and size distributions), with a ratio of primary to secondary particles similar to those found in a typical coal-fired power plant plumes. Additionally, overall concentrations appear to be comparable to those reported in previous toxicological studies that used concentrated air particles (Batalha et al., 2002; Clarke et al., 2000; Wellenius et al., 2003). Another paper (Ruiz et al., 2007) includes an overall description of the exposure system to study coal-fired power plant emissions. In that article the test aerosols produced by simulating different atmospheric scenarios are characterized. This system can be used to compare the toxicity of primary and secondary particles from coal-fired power plant emissions, and to compare emissions from different power plants.

REFERENCES

- Batalha, J. R. F., Saldiva, P. H. N., Clarke, R. W., Coull, B. A., Stearns, R. C., Lawrence, J., Murthy, G. G. K., Koutrakis, P., and Godleski, J. J. 2002. Concentrated ambient air particles induce vasoconstriction of small pulmonary arteries in rats. *Environ. Health Perspect.* 110:1191–1197.
- Clarke, R. W., Coull, B., Reinisch, U., Catalano, P., Killingsworth, C. R., Koutrakis, P., Kavouras, I., Murthy, G. G. K., Lawrence, J., Lovett, E., Wolfson, J. M., Verrier, R. L., and Godleski, J. J. 2000. Inhaled concentrated ambient particles are associated with hematologic and bronchoalveolar lavage changes in canines. *Environ. Health Perspect.* 108:1179–1187.
- Cocker, D. R., Flagan, R. C., and Seinfeld, J. H. 2001. State-of-the-art chamber facility for studying atmospheric aerosol chemistry. *Environ. Science & Technol.* 35:2594–2601.
- Crump, J. G., and Seinfeld, J. H. 1981. Turbulent deposition and gravitational sedimentation of an aerosol in a vessel of arbitrary shape. *J. Aerosol Sci.* 12:405–415.
- Dockery, D. W., and Pope, C. A. 1994. Acute respiratory effects of particulate air pollution. *Annu. Rev. Public Health* 15:107–132.
- Dockery, D. W., Pope, C. A., Xu, X. P., Spengler, J. D., Ware, J. H., Fay, M. E., Ferris, B. G., and Speizer, F. E. 1993. An association between air pollution and mortality in 6 United States cities. *N. Engl. J. Med.* 329:1753–1759.
- Finlayson-Pitts, B. J., and Pitts, J. N. 2000. *Chemistry of the upper and lower atmosphere*. San Diego, CA: Academic Press.
- Hewitt, C. N. 2001. The atmospheric chemistry of sulphur and nitrogen in power station plumes. *Atmos. Environ.* 35:1155–1170.
- Holmes, M. G. 2002. An outdoor multiple wavelength system for the irradiation of biological samples: Analysis of the long-term performance of various lamp and filter combinations. *Photochem. Photobiol.* 76:158–163.
- Kodavanti, U. P., Hauser, R., Christiani, D. C., Meng, Z. H., Mcgee, J., Ledbetter, A., Richards, J., and Costa, D. L. 1998. Pulmonary responses to oil fly ash particles in the rat differ by virtue of their specific soluble metals. *Toxicol. Sci.* 43:204–212.
- Kodavanti, U. P., Schladweiler, M. C., Ledbetter, A. D., Hauser, R., Christiani, D. C., Mcgee, J., Richards, J. R., and Costa, D. L. 2002. Temporal association between pulmonary and systemic effects of particulate matter in healthy and cardiovascular compromised rats. *J. Toxicol. Environ. Health A* 65:1545–1569.
- Koutrakis, P., Wolfson, J. M., Slater, J. L., Brauer, M., Spengler, J. D., Stevens, R. K., and Stone, C. L. 1988. Evaluation of an annular denuder filter pack system to collect acidic aerosols and gases. *Environ. Sci. Technol.* 22:1463–1468.
- Luria, M., Olszyna, K. J., and Meagher, J. F. 1983. The atmospheric oxidation of flue-gases from a coal-fired power-plant—A comparison between smog chamber and airborne plume sampling. *J. Air Pollut. Control Assoc.* 33:483–487.
- Luria, M., Stockburger, L., Olszyna, K. J., and Meagher, J. F. 1982. Dynamics of sulfate particle-production and growth in smog chamber experiments. *Atmos. Environ.* 16:697–708.
- McDonald, J. D., Harrod, K. S., Seagrave, J. C., Seilkop, S. K., and Mauderly, J. L. 2004. Effects of low sulfur fuel and a catalyzed particle trap on the composition and toxicity of diesel emissions. *Environ. Health Perspect.* 112:1307–1312.
- McLeod, A. R. 1997. Outdoor supplementation systems for studies of the effects of increased UV-B radiation. *Plant Ecol.* 128:78–92.
- McMurry, P. H., and Rader, D. J. 1985. Aerosol wall losses in electrically charged chambers. *Aerosol Sci. Technol.* 4:249–268.
- Mentel, T. F., Bleilebens, D., and Wahner, A. 1996. A study of nighttime nitrogen oxide oxidation in a large reaction chamber—The fate of NO_2 , N_2O_5 , HNO_3 , and O^{-3} at different humidities. *Atmos. Environ.* 30:4007–4020.
- Peters, T. M., Chein, H. M., Lundgren, D. A., and Keady, P. B. 1993. Comparison and combination of aerosol-size distributions measured with a low-pressure impactor, differential mobility particle sizer, electrical aerosol analyzer, and aerodynamic particle sizer. *Aerosol Sci. Technol.* 19:396–405.

- Pope, C. A., Thun, M. J., Namboodiri, M. M., Dockery, D. W., Evans, J. S., Speizer, F. E., and Heath, C. W. 1995. Particulate air pollution as a predictor of mortality in a prospective study of US adults. *Am. J. Respir. Crit. Care Med.* 151:669–674.
- Reed, M. D., Gigliotti, A. P., McDonald, J. D., Seagrave, J. C., Seilkop, S. K., and Mauderly, J. L. 2004. Health effects of subchronic exposure to environmental levels of diesel exhaust. *Inhal. Toxicol.* 16:177–193.
- Ruiz, P. A., Gupta, T., Kang, C.-M., Lawrence, J. E., Ferguson, S. T., Wolfson, J. M., Rohr, A. C., and Koutrakis, P. 2007. Development of an exposure system for the toxicological evaluation of particles derived from coal-fired power plants. *Inhal. Toxicol.* 19:607–619.
- Seinfeld, J. H., and Pandis, S. N. 1998. *Atmospheric chemistry and physics*. New York: John Wiley and Sons.
- Stockwell, W. R., and Calvert, J. G. 1983. The mechanism of the HO-SO₂ reaction. *Atmos. Environ.* 17:2231–2235.
- Wahner, A., Mentel, T. F., and Sohn, M. 1998. Gas-phase reaction of N₂O₅ with water vapor: Importance of heterogeneous hydrolysis of N₂O₅ and surface desorption of HNO₃ in a large Teflon chamber. *Geophys. Res. Lett.* 25:2169–2172.
- Wellenius, G. A., Saldiva, P. H. N., Batalha, J. R. F., Murthy, G. G. K., Coull, B. A., Verrier, R. L., and Godleski, J. J. 2002. Electrocardiographic changes during exposure to residual oil fly ash (ROFA) particles in a rat model of myocardial infarction. *Toxicol. Sci.* 66:327–335.
- Wellenius, G. A., Coull, B. A., Godleski, J. J., Koutrakis, P., Okabe, K., Savage, S. T., Lawrence, J. E., Murthy, G. G. K., and Verrier, R. L. 2003. Inhalation of concentrated ambient air particles exacerbates myocardial ischemia in conscious dogs. *Environ. Health Perspect.* 111:402–408.

Copyright of Inhalation Toxicology is the property of Taylor & Francis Ltd and its content may not be copied or emailed to multiple sites or posted to a listserv without the copyright holder's express written permission. However, users may print, download, or email articles for individual use.